COMPUTATIONAL BIOLOGY

Decoupling of Receptor and Downstream Signals in the Akt Pathway by Its Low-Pass Filter Characteristics

Kazuhiro A. Fujita,[1] Yu Toyoshima,[2] Shinsuke Uda,[2] Yu-ichi Ozaki,[2] Hiroyuki Kubota,[2] Shinya Kuroda[1,2]*

(Published 27 July 2010; Volume 3 Issue 132 ra56)

In cellular signal transduction, the information in an external stimulus is encoded in temporal patterns in the activities of signaling molecules; for example, pulses of a stimulus may produce an increasing response or may produce pulsatile responses in the signaling molecules. Here, we show how the Akt pathway, which is involved in cell growth, specifically transmits temporal information contained in upstream signals to downstream effectors. We modeled the epidermal growth factor (EGF)–dependent Akt pathway in PC12 cells on the basis of experimental results. We obtained counterintuitive results indicating that the sizes of the peak amplitudes of receptor and downstream effector phosphorylation were decoupled; weak, sustained EGF receptor (EGFR) phosphorylation, rather than strong, transient phosphorylation, strongly induced phosphorylation of the ribosomal protein S6, a molecule downstream of Akt. Using frequency response analysis, we found that a three-component Akt pathway exhibited the property of a low-pass filter and that this property could explain decoupling of the peak amplitudes of receptor phosphorylation and that of downstream effectors. Furthermore, we found that lapatinib, an EGFR inhibitor used as an anticancer drug, converted strong, transient Akt phosphorylation into weak, sustained Akt phosphorylation, and, because of the low-pass filter characteristics of the Akt pathway, this led to stronger S6 phosphorylation than occurred in the absence of the inhibitor. Thus, an EGFR inhibitor can potentially act as a downstream activator of some effectors.

INTRODUCTION

In communication systems, information is often encoded as temporal patterns of signals, and signals are selectively transmitted and decoded by the characteristics of signal processing modules (*1*). In cellular signal transduction, information is also encoded as temporal patterns of the activities of signaling molecules and is selectively transmitted and decoded by characteristics of the signal transduction pathways, leading to specific cellular responses (*2*–*6*). The characteristics of these signal transduction pathways have been analyzed in an effort to elucidate the frequency responses of various cellular processes (*7*–*9*). Although periodic stimuli are generally used for frequency response analyses, producing periodic stimuli can be technically difficult. Therefore, instead of using periodic stimuli, we decomposed the time courses of the phosphorylation of signaling molecules into frequency waves with a Fourier transform and examined the signal transfer efficiency from receptors to downstream molecules.

The activity of Akt [also known as protein kinase B (PKB)] is stimulated by various growth factors, and this serine-threonine kinase plays evolutionarily conserved roles in many cellular functions, such as protein synthesis and cell growth (*10*, *11*). In the rat pheochromocytoma cell line PC12, Akt signaling regulates cell growth in response to growth factors, including epidermal growth factor (EGF) (*12*–*15*). The binding of growth factors to their receptors leads to the activation of phosphatidylinositol 3-kinase (PI3K) and the subsequent phosphorylation and activation of Akt. Akt stimulates downstream molecules, such as S6 kinase, through the mammalian target of rapamycin (mTOR) complex 1, and activated S6 kinase phosphorylates ribosomal protein S6 (*16*–*20*), which is consistent with the role of S6 regulating cell size (*21*, *22*). Despite knowledge of the outcomes of Akt signaling, the temporal coding in the Akt pathway remains to be elucidated.

Here, we found a counterintuitive decoupling of peak amplitudes between receptor phosphorylation and phosphorylation of downstream effectors; a weak sustained phosphorylation of the EGF receptor (EGFR), rather than a strong transient phosphorylation, strongly induced the phosphorylation of S6. Thus, the signal transfer efficiency in the Akt pathway depends on the temporal pattern of receptor phosphorylation. With a frequency response analysis of a three-component Akt pathway model, we identified a low-pass filter characteristic of this Akt pathway. Because the higher-frequency waves were not efficiently transferred downstream compared with the lower-frequency waves, the Akt pathway can decouple the peak amplitudes of receptor phosphorylation and downstream effector phosphorylation. Furthermore, we found that through this decoupling effect, lapatinib, an EGFR inhibitor used as an anticancer drug, acted as a downstream activator of one effector.

RESULTS

Decoupling in the Akt pathway activated by EGF in PC12 cells

We measured the time courses of phosphorylated EGFR (pEGFR), phosphorylated Akt (pAkt), and phosphorylated S6 (pS6) in response to step stimulation of PC12 cells with EGF (Fig. 1, A and B, left columns, and fig. S1). We then developed a simple schematic simulation model of this three-

[1]Department of Computational Biology, Graduate School of Frontier Sciences, University of Tokyo, Kshiwanoha 5-1-5, Kashiwa, Chiba 277-8568, Japan. [2]Department of Biophysics and Biochemistry, Graduate School of Science, CREST, Japan Science and Technology Agency, University of Tokyo, Hongo 7-3-1, Bunkyo-ku,Tokyo 113-0033, Japan.
*To whom correspondence should be addressed. E-mail: skuroda@bi.s.u-tokyo.ac.jp

component (EGFR, Akt, S6) EGF-dependent Akt pathway (Fig. 2) and fitted the parameters of the model with the experimental data from cells responding to step stimulation (Fig. 1, B and C, and fig. S2). Hereafter, this simple schematic model is referred to as the "Akt pathway model." To test the validity of this model, we predicted the responses of this three-component Akt pathway to pulse and ramp stimulation with EGF (Fig. 1, A and C, center and right columns) and validated the predicted responses experimentally (Fig. 1B and fig. S3). The Akt pathway model quantitatively characterized the time courses of pEGFR, pAkt, and pS6 in response to step, pulse, and ramp stimulation with EGF (Fig. 1, B and C), indicating that the Akt pathway model is valid. The responses in this Akt pathway to step, pulse, and ramp stimulations were distinct. Hereafter, a transient time course refers to a rapid response in which the peak occurred within 5 min of stimulation, and a sustained time course refers to a slow response in which the peak occurred after 5 min.

Step stimulation with EGF produced strong transient and weak sustained time courses of pEGFR and pAkt (Fig. 1B). Pulse stimulation with EGF produced only strong transient time courses of pEGFR and pAkt. Ramp stimulation with EGF produced mainly a sustained time course of pEGFR and pAkt. The peak amplitudes of pEGFR and pAkt produced by step and pulse stimulations were similar and larger than those produced by ramp stimulation. In all stimulation paradigms, the time course of pS6 was different from the time courses of pEGFR and pAkt; pS6 exhibited a sustained time course. The peak amplitude of pS6 by step stimulation was larger than that produced by pulse stimulation, despite the similar peak amplitudes of pAkt observed in response to either step or pulse stimulation. The peak amplitude of pS6 produced by ramp stimulation with EGF was similar to that produced by step stimulation. Here, we denote dose response as the amount of phosphorylation produced by EGF concentrations at the indicated time. The dose response of pS6 at 30 min produced by step stimulation was convex and reached a maximum at an EGF concentration of 1 ng/ml, whereas that by pulse stimulation was monotonic, steadily increasing with increasing concentrations of EGF (fig. S3). The time course of phosphorylated S6 kinase, an intermediate molecule between Akt and S6, showed an intermediate time course pattern between that of pAkt and that of pS6 (fig. S4).

The Akt pathway model reproduced the above features of the experimental results (Fig. 1C), indicating that the Akt pathway model can capture the systems-level dynamics of this Akt pathway in PC12 cells. We had initially tried to develop a complex signaling pathway model that included cross talk and feedback, but found that even the simple Akt pathway model sufficiently reproduced the experimental results. Moreover, phosphorylation of S6 is mainly dependent on the Akt pathway in PC12 cells (*23*), and we confirmed that the addition of LY294002 and rapamycin, inhibitors of PI3K and mTOR, respectively, completely inhibited S6 phosphorylation in PC12 cells (fig. S5). Together, these results indicate that, at least in PC12 cells, S6 phosphorylation is mainly dependent on the Akt pathway. Therefore, we used the Akt pathway model to elucidate the temporal coding mechanisms at the systems level. Note that the Akt pathway model was built by lumping molecular species and reactions together into abstracted variables to distill the essential characteristics of signal transduction dynamics and was not intended to describe the detailed molecular reactions (*24*).

Intuitively, one may think that peak amplitudes of upstream and downstream molecules would correlate; however, we obtained counterintuitive phosphorylation kinetics by immunoblotting (Fig. 1D). Despite a much larger peak amplitude of pEGFR in response to pulse stimulation than that produced by ramp stimulation, the peak amplitude of pS6 by ramp stimulation was much larger than that by pulse stimulation (Fig. 1D). Furthermore, despite the similar peak amplitudes of pEGFR produced by step and

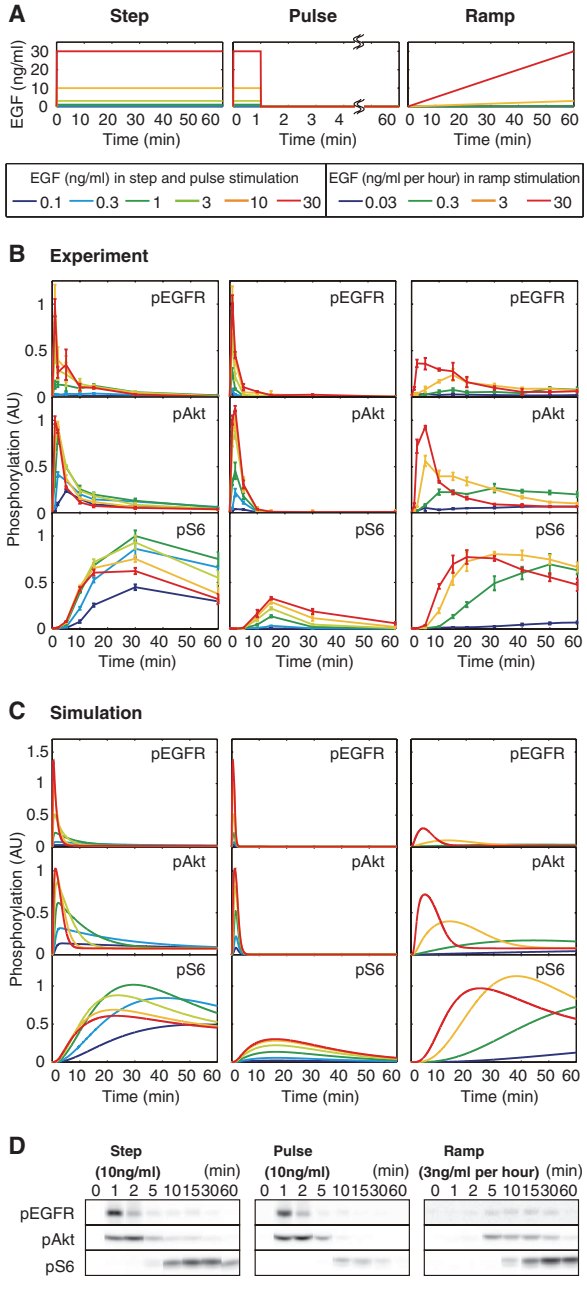

Fig. 1. EGF-dependent dynamics of the Akt pathway. (**A**) Step, pulse, and ramp stimulation with EGF performed in the experiments and simulations. The concentrations of EGF used for the step and pulse stimulations were the same and are indicated in the key; the pulse stimulation was 1 min in duration. The rate of increase for the ramp stimulation is indicated in the key. (**B**) EGF-induced time courses of pEGFR, pAkt, and pS6 in PC12 cells by step (left column), pulse (middle column), and ramp (right column) stimulation. The means and SEM of three independent experiments are shown. The doses and time courses of EGF are shown in (A). Images of the original immunoblot gels and S6 kinase phosphorylation are shown in fig. S1. AU, arbitrary unit. (**C**) EGF-induced pEGFR, pAkt, and pS6 in the Akt pathway model by step (left column), pulse (middle column), and ramp (right column) stimulation. (**D**) Images of original immunoblots of pEGFR, pAkt, and pS6 by step (10 ng/ml), pulse (10 ng/ml for 1 min), and ramp (3 ng/ml per hour) stimulation.

pulse stimulations, the peak amplitude of pS6 by pulse stimulation was much lower than that produced by step stimulation (Fig. 1D). Thus, even a strong, transient time course of pEGFR poorly induced pS6, whereas a weak sustained time course of pEGFR strongly induced pS6. These counter-intuitive characteristics were conserved throughout all the temporal patterns of stimulation that were tested (Fig. 1B). We refer to this phenomenon, in which the relationship of the magnitude of the peak amplitudes of the time courses of upstream molecules is opposite to that of downstream molecules, as "decoupling." The phenomenon in which the relationship of the magnitude of the peak amplitudes of the time courses of upstream molecules is the same as that of downstream molecules is referred to as "coupling." Thus, the peak amplitudes of transient and sustained time courses between upstream and downstream molecules can be decoupled in the Akt pathway (Fig. 1D).

If only the responses to pulse stimulation are considered, one may think that the relationship of the peak amplitudes between pAkt and pS6 is always coupled, because the appearance of pS6 looks like a delayed and decayed pAkt response. Furthermore, in response to pulse stimulation, the dose responses of both pAkt at 1 min and pS6 at 30 min were monotonic (fig. S3). By step stimulation, however, the dose response of pAkt at 1 min was monotonic (fig. S3), whereas that of pS6 at 30 min was convex (Fig. 1, B and C, and fig. S3). This observation indicates that the conversion of the time course of pAkt to that of pS6 is not a simple delay and decay response. By step stimulation, the dose response of pAkt at 30 min was convex, similar to the pS6 response (fig. S3), suggesting that this sustained time course of pAkt, rather than the transient time course, was responsible for the convex dose response of pS6. Thus, as the signal descends from pAkt to pS6, the transient time course seems to be relatively decayed compared with the sustained time course, resulting in the convex dose response of pS6 (fig. S3). Consistently, the sustained time course of pAkt was relatively enhanced by ramp stimulation (Fig. 1, B and C). These results suggest that the signal transfer efficiency from the upstream molecule to the downstream molecule differs depending on the shapes of the time courses.

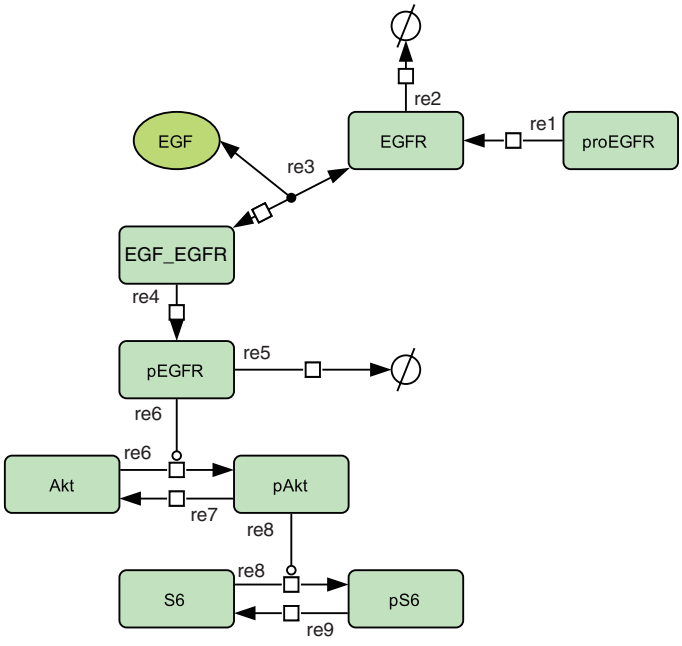

Fig. 2. Schematic of the simple simulation model of the EGF-dependent Akt pathway. The schematic was created with CellDesigner (*43*). Arrows indicate biochemical reaction. The circle with a line through it represents degradation, a box on an edge represents a direction of chemical reaction, and a circle connecting an edge to a box on an edge represents an enzymatic reaction.

Frequency response analysis of the Akt pathway

To examine the signal transfer efficiency of transient and sustained time courses, we used a frequency response analysis, which is often used in fields such as analog communication systems (*1*). An outline and an explanation of the concepts involved in the frequency response analysis used in this study are summarized in Fig. 3 and fig. S6A, respectively. Periodic stimuli are generally used for frequency response analyses. Because of the technical difficulties in producing periodic stimuli, we decomposed the time courses of the phosphorylation of the signaling molecules into frequency waves with a Fourier transform and examined the signal transfer efficiency from receptors to downstream molecules by dividing the amplitudes of the frequency waves of the downstream molecules by those of the upstream molecules (Fig. 3 and fig. S6A; see Materials and Methods).

To examine the signal transfer efficiencies of typical transient and sustained time courses of pEGFR induced by pulse (10 ng/ml for 1 min) or ramp (3 ng/ml per hour) stimulation, respectively, we obtained amplitude spectra (Fig. 4 and fig. S7A) of the time courses of pEGFR, pAkt, and pS6 in the Akt pathway model by performing a Fourier transform. We used the simulated time courses for the frequency response analysis instead of the experimental time courses because of the experimental difficulty in obtaining the short interval (1 s) required for a Fourier transform. The amplitude spectrum of a time course consists of the amplitudes of the frequency waves that constitute the time course and can be obtained by decomposing the time course into frequency waves with a Fourier transform (fig. S6, B and C). From the experimental and simulation data, it is clear that as the signal descended from pEGFR to pS6, the signal of the transient time course decayed compared with that of the sustained time course (Fig. 4A). The peak amplitude of the transient time course of pEGFR was higher than that of the sustained time course. Similarly, the peak amplitude of the transient time course of pAkt was higher than that of the sustained time course. In contrast, the peak amplitude of the sustained time course of pS6 was higher than that of the transient time course. Thus, the relationship between the peak amplitudes of the transient and sustained time courses of pEGFR and pAkt was coupled, whereas that between the peak amplitudes of pAkt and pS6 was decoupled.

When these data are converted by Fourier transform, at higher frequencies (about $>2 \times 10^{-3}$), the amplitudes of the amplitude spectrum of the transient time course of pEGFR were larger than the amplitudes of the sustained time course, whereas at lower frequencies (about $<2 \times 10^{-3}$), the amplitudes of the sustained time course were larger than those of the transient time course (Fig. 4B). The amplitude spectra for pAkt and pS6 showed a relationship between the sustained and transient time courses similar to that of pEGFR. The amplitudes of pEGFR at higher frequencies were larger than those of pAkt, and those of pAkt were larger than those of pS6. The amplitudes of pEGFR at lower frequencies were smaller than those of pAkt, and those of pAkt were smaller than those of pS6. This indicates that amplitudes at higher frequencies became smaller, whereas those at lower frequencies became larger, as the signal descended from pEGFR to pS6. This suggests that as the signal descends downstream, the transient time course becomes relatively decayed compared with the sustained time course because the amplitudes of the transient time course of pEGFR at a higher frequency are larger than those of the sustained time course. This phenomenon may decouple the peak amplitudes of pEGFR from those of downstream molecules. We examined the amplitude spectra of pEGFR,

pAkt, and pS6 (Fig. 1) and obtained similar results; that is, the amplitudes at higher frequencies were relatively decayed downstream, compared with those at lower frequencies, regardless of the stimulation patterns (fig. S7A). These results raised the possibility that the Akt pathway exhibited the properties of a low-pass filter.

Signal transfer efficiency of the Akt pathway

To examine the low-pass filter properties of the Akt pathway, we divided the amplitude spectrum of the downstream molecule by that of the upstream molecule. This ratio corresponds to the frequency-dependent signal transfer efficiency from the upstream molecule to the downstream molecule (see Materials and Methods and fig. S6D). This ratio was defined as the "frequency-dependent gain." Although the frequency-dependent gains from pEGFR to pAkt differed slightly depending on the doses of EGF, overall, the frequency-dependent gains of both pEGFR-to-pAkt and pAkt-to-pS6 pathways became constant at lower frequencies and began to attenuate at higher frequencies (Fig. 5A). This outcome means that the signal transfer efficiency at lower frequencies is better than that at higher frequencies. Thus, this frequency-dependent gain resembles that of a low-pass filter, which means that the system will transmit slowly occurring changes in upstream signals to produce a downstream response, but cannot efficiently transmit rapidly occurring changes in upstream signals. Moreover, similar

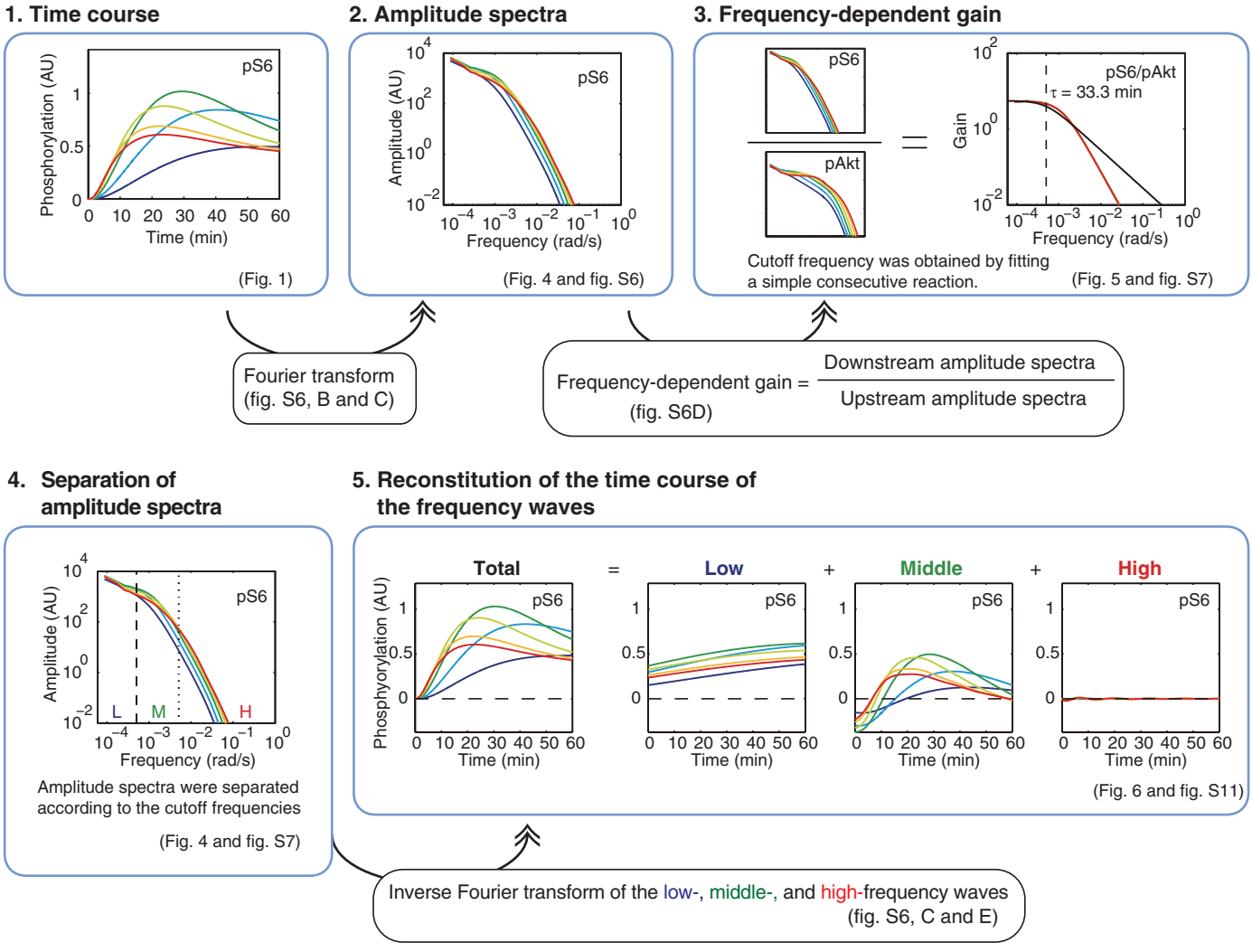

Fig. 3. Procedures of frequency response analysis used in this study. The workflow from the time course of the Akt pathway model (Fig. 1) to the reconstituted time courses composed of the low-, middle-, and high-frequency waves (Fig. 6 and fig. S6) is summarized. The time courses of the signaling molecules in the Akt pathway model were decomposed into frequency waves with a Fourier transform, and the amplitude spectra of each signaling molecule were obtained (Fig. 4 and fig. S7). The amplitude spectra of the downstream molecules were divided by those of the upstream molecules, and the frequency-dependent gain, which reflects the signal transfer efficiency, was obtained (Fig. 5 and fig. S7). The cutoff frequencies, above which a gain rapidly attenuates, were obtained by fitting the frequency-dependent gain as a simple consecutive reaction (Fig. 5). On the basis of the cutoff frequency of the pEGFR→pAkt step and the pAkt→pS6 step in the pathway, the amplitude spectra were separated into low-, middle-, and high-frequency bands (Fig. 4 and fig. S7). The time course composed of the low-, middle-, and high-frequency waves was reconstituted with an inverse Fourier transform of the separated amplitude spectra (Fig. 6 and fig. S11). A corresponding detailed description of each procedure can be found in fig. S6.

frequency-dependent gains for both pEGFR to pAkt and from pAkt to pS6 were obtained regardless of the temporal patterns of the stimulation (fig. S7B).

One of the indices of the characteristics of a low-pass filter is a cutoff frequency, which is the inverse of a time constant. Frequency waves higher than the cutoff frequency are less efficiently transferred downstream than frequency waves lower than the cutoff frequency. A simple consecutive reaction, one of the simplest biochemical reactions and linear time-invariant systems, is a typical low-pass filter (fig. S6, A and D). Therefore, we fitted pEGFR→pAkt and pAkt→pS6 in the Akt pathway model as simple consecutive reactions (Fig. 5A, black lines, and figs. S7B and S8) and found that the overall responses of pEGFR, pAkt, and pS6 to step, pulse, and ramp stimulations with EGF were reasonably fitted (fig. S8). This indicates that the Akt pathway can be regarded as a linear time-invariant system under the above conditions. By fitting the Akt pathway models with simple consecutive reactions, we obtained the apparent cutoff frequency of the pathways (Fig. 5A, dotted and dashed lines). The cutoff frequencies of the fitted consecutive reactions for pEGFR to pAkt and pAkt to pS6 were 1/3.27 and 1/33.3 rads/min, respectively.

To verify the low-pass filter characteristic of the Akt pathway in another context, we also modeled a simple three-component Akt pathway activated by nerve growth factor (NGF) in PC12 cells (figs. S9 and S10). We observed characteristics similar to those of low-pass filters in this NGF-activated Akt pathway despite differences between the temporal patterns of phosphorylated TrkA (pTrkA), one of the subunits of NGF receptors, and those of pEGFR (fig. S9). The time courses of pTrkA were transient and sustained, and the amplitude of the sustained time course was much larger than that of pEGFR (fig. S9A). The cutoff frequencies of the fitted consecutive reactions of pTrkA to pAkt and pAkt to pS6 in response to NGF were 1/0.849 and 1/55.4 rads/min, respectively (fig. S10). This result indicates that the Akt pathway similarly functions as a low-pass filter regardless of the distinct temporal patterns of the phosphorylated EGF and NGF receptors in PC12 cells. However, the Akt pathway may not function as a low-pass filter in other cell lines or downstream of other types of receptors where one or more additional signaling pathways or cross talk regulates the Akt pathway.

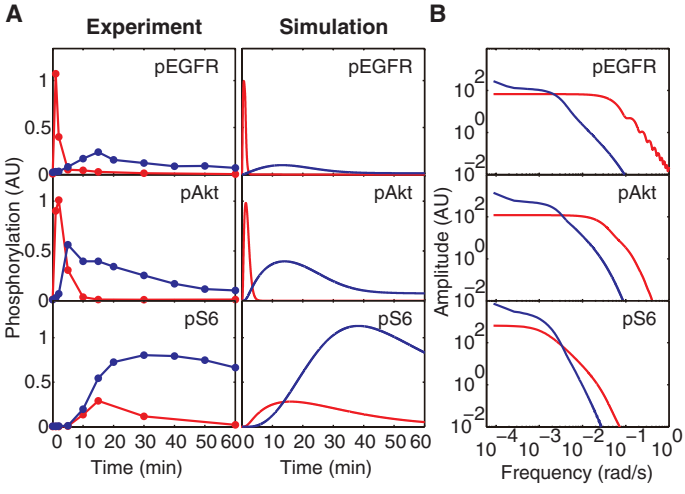

Fig. 4. Transient and sustained pEGFR and downstream phosphorylation. (A) Transient (red) and sustained (blue) time courses of pEGFR were induced by pulse (10 ng/ml for 1 min) or ramp (3 ng/ml per hour) stimulation, respectively. (B) Amplitude spectra of pEGFR, pAkt, and pS6. The red and blue lines represent the transient and sustained responses, respectively. The frequency unit is angular frequency (radians per second). Both axes are plotted on logarithmic scales.

For the EGF-activated Akt pathway, we separated the frequency domain into high- and middle-frequency bands according to the cutoff frequencies of pEGFR to pAkt and into middle- and low-frequency bands according to the cutoff frequency of pAkt to pS6 (Fig. 5B). The waves of pEGFR within the low-frequency (Fig. 5B, blue) and middle-frequency bands (Fig. 5B, green), both of which were below the cutoff frequency of pEGFR to pAkt, were efficiently transferred to pAkt. However, the waves within the high-frequency band (Fig. 5B, red) were not efficiently transferred to pAkt because of the nature of the low-pass filter. Similarly, the waves of pAkt within the low-frequency band, which was below the cutoff frequency of pAkt to pS6, were efficiently transferred to pS6, and the waves of pAkt within the middle- and high-frequency bands were not (Fig. 5B). Thus, the waves of pEGFR within the low-frequency band, which was below the cutoff frequencies of both pEGFR to pAkt and pAkt to pS6, were most efficiently transferred to pS6. We set the amplitude of each frequency wave of pEGFR at 1 so that the y axes of pAkt and pS6 directly reflect the gain of each step. The gains of pAkt and pS6 for the low-frequency waves were 2.59 and 8.31, respectively, indicating signal amplification. The gains reflect the value of pEGFR, pAkt, and pS6, whose peak intensities were normalized at 1 in Fig. 1. Therefore, the values of the gains were arbitrary and did not indicate the physiologically meaningful amplification or attenuation of the signals (Fig. 5B).

Frequency filtration in the Akt pathway

To understand why the weak sustained time course of pEGFR induced pS6 more strongly than did the strong transient time course (Fig. 4), we separated the original time courses of pEGFR, pAkt, and pS6 according to the corresponding frequency bands and examined the transfer efficiencies of these time courses (Fig. 6). Using an inverse Fourier transform of the corresponding spectra, we reconstituted the time courses into low-, middle- and high-frequency waves (figs. S6E and S7A). The sum of the time courses of the low-, middle-, and high-frequency waves equaled that of the original time course.

In the transient time course of pEGFR, the time course of the high-frequency waves was dominant compared with the time courses for the other frequency waves (Fig. 6, upper row, red). In the sustained time course of pEGFR, the time course of the middle-frequency waves, rather than the high-frequency waves, was dominant (Fig. 6, upper row, blue). Although not apparent at the scale shown in Fig. 6, there were low-frequency waves in the sustained time course of pEGFR. As the signal descended from pEGFR to pAkt, the time courses of the low- and middle-frequency waves were transferred more efficiently than the time course of the high-frequency waves, which was above the cutoff frequency of pEGFR to pAkt (Fig. 6, upper and middle rows). As the signal descended from pAkt to pS6, the time course of the low-frequency waves was transferred more efficiently than the time courses of the middle- and high-frequency waves, which were above the cutoff frequency of pAkt to pS6 (Fig. 6, middle and lower rows). In the time course of pS6, in particular, the time course of the high-frequency waves almost completely disappeared and that of the low-frequency waves became dominant (Fig. 6, lower row). Because the transient time course of pEGFR was mainly composed of high-frequency waves, the transient time course of pEGFR was not efficiently transferred downstream. In contrast, the sustained time course of pEGFR was mainly composed of middle-frequency waves and a small amount of low-frequency waves, both of which were efficiently transferred downstream to pAkt. Middle-frequency waves were dominant in the sustained time course of pAkt but were not efficiently transferred to pS6. In the sustained time

course of pS6, both middle- and low-frequency waves were dominant. Thus, weak low-frequency waves in the sustained time course of pEGFR became dominant in the sustained time course of pS6. Therefore, the difference in the transfer efficiencies of the transient and sustained time courses depended on the "high-frequency cutoff" characteristics of the low-pass filters of the Akt pathway. We observed these characteristics of the Akt pathway regardless of the temporal stimulation pattern (fig. S11). Hence, the stimulation conditions that produced sustained time courses contained more low-frequency waves than those stimulations that produced predominantly transient time courses, and the low-pass filter properties of the pathway meant that stimulations that produced waves below this frequency were more effective at activating pS6. For this reason, the Akt pathway is capable of decoupling the relationship between the peak amplitudes of the transient and sustained time courses of upstream and downstream molecules, such that even a weak sustained time course of pEGFR induced by ramp stimulation induced pS6 more strongly than did a strong transient time course induced by pulse stimulation (Figs. 1D, 4, and 6). In addition, although step and pulse stimulation induced similar peak amplitudes of pEGFR and pAkt, only step stimulation, and not pulse stimulation, strongly induced pS6. This phenomenon can be explained by the fact that only step stimulation, and not pulse stimulation, induced sustained time courses of pEGFR and pAkt (Fig. 1).

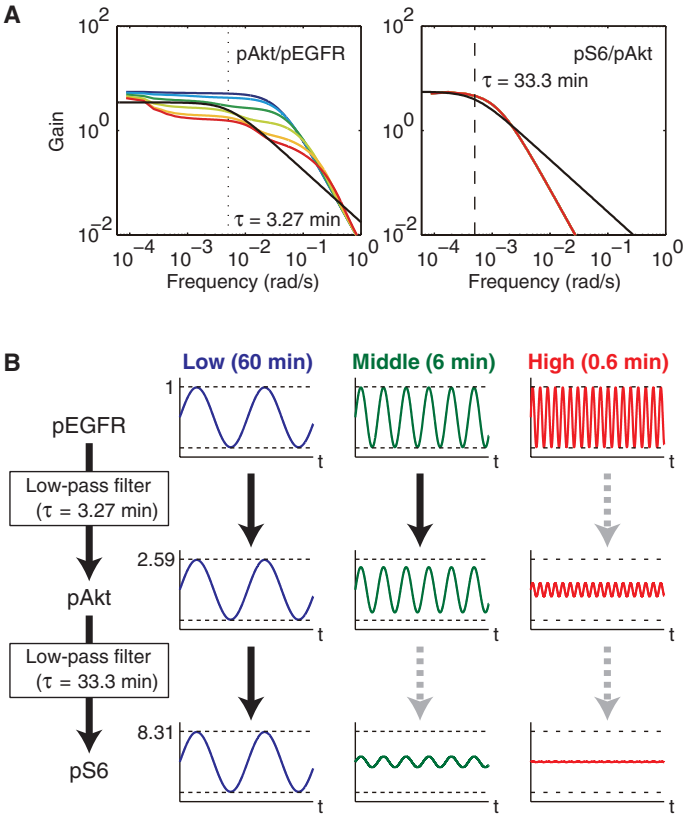

Fig. 5. Signal transfer efficiency of the Akt pathway. (A) Frequency-dependent gains of the pEGFR→pAkt (left panel) and pAkt→pS6 (right panel) portions of the pathway by step stimulation. The colors indicate that the data are from different concentrations of EGF and are described in Fig. 1A. The black lines indicate the fitted simple consecutive reactions of the pEGFR→pAkt and pAkt→pS6 parts of the pathway. The cutoff frequency of the fitted consecutive reaction of the part of the pathway is indicated by a dotted or dashed line. The cutoff frequency is the inverse of the time constant τ. (B) Transfer efficiencies of the low-, middle-, and high-frequency waves of the fitted consecutive reactions. We set the amplitude of each frequency wave of pEGFR at 1 so that the *y* axes of pAkt and pS6 directly reflect the gain of each step. The gains of pAkt and pS6 for the low-frequency waves were 2.59 and 8.31, respectively, indicating the signal amplification. The gains reflect the value of pEGFR, pAkt, and pS6, whose peak intensities were normalized at 1 in Fig. 1.The *x* axes denote time and were scaled differently for each wave to fit the size of each panel.

Conversion of EGFR inhibitor to a downstream activator by the low-pass filter characteristic of the Akt pathway

The fact that a weak sustained time course of pEGFR induced pS6 more strongly than a strong transient time course raises the possibility that an inhibitor may convert a strong transient time course of an upstream molecule into a weak sustained time course; thus, the inhibitor could be a downstream activator. To examine this possibility, we examined the effect of lapatinib, a selective EGFR inhibitor (tyrosine kinase inhibitor) used as a clinical anticancer drug (*25*, *26*), on EGF-dependent phosphorylation in PC12 cells (Fig. 7). Lapatinib inhibited the phosphorylation of EGFR in a dose-dependent manner, as previously reported (*25*) (Fig. 7A, upper panel). The inhibitor also inhibited the transient phosphorylation of Akt (1 min after addition of EGF), but it prolonged and enhanced the phosphorylation of Akt at 30 min after addition of EGF (Fig. 7, A, middle panel, and C). Thus, the inhibitor converted a strong transient time course of Akt phosphorylation into a weak sustained time course. At longer time points (>60 min), the presence of the inhibitor resulted in a greater EGF-dependent phosphorylation of S6 than occurred in its absence (Fig. 7, A and C). We observed this promotion of downstream signaling by the inhibitor for a wide range of concentrations (15 to 150 nM) above the IC_{50} [half maximal (50%) inhibitory concentration] of the inhibitor (10.2 nM) (*25*) (Fig. 7A, lower panel), suggesting that at these concentrations, lapatinib can potentiate some signaling events downstream of the receptor. A higher dose of the inhibitor (500 nM) inhibited S6 phosphorylation (Fig. 7A, lower panel, dark blue

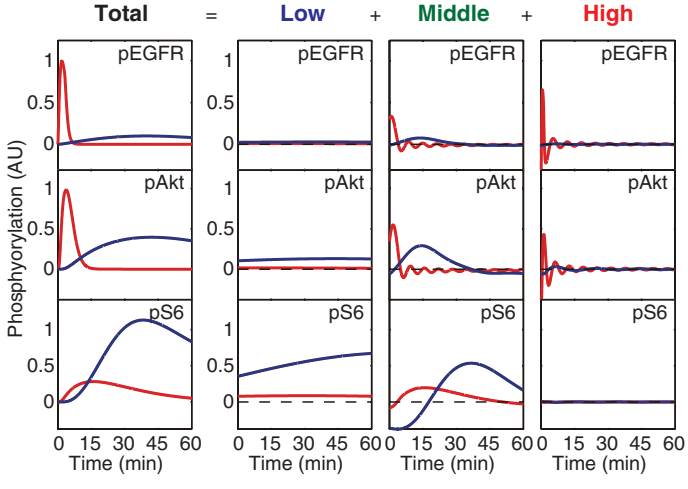

Fig. 6. Frequency filtration of receptor phosphorylation through the Akt pathway. Transient (red) or sustained (blue) time course of pEGFR can be separated into the time courses of the low-, middle-, and high-frequency waves. The time courses of the frequency waves are mathematically separated and contain negative values.

line). Therefore, the effect of the inhibitor on S6 phosphorylation was convex; middle doses of the inhibitor (15 to 150 nM) were most effective in S6 phosphorylation at 60 min (Fig. 7A). By including the kinetics of the inhibitor reactions with EGFR into the Akt pathway model (fig. S12), the model reproduced many features of the experimental results, particularly the inhibitor-mediated conversion of the transient time course of pAkt into a sustained time course and the convex effect of the inhibitor on pS6 (Fig. 7B). Because of the conversion of the transient time course of pAkt into a sustained one by the inhibitor and the low-pass filter characteristic of the Akt pathway, EGF in the presence of the EGFR inhibitor induced pS6 more strongly than in the absence of the inhibitor, which meant that the inhibitor served as an activator of the Akt-dependent downstream effector.

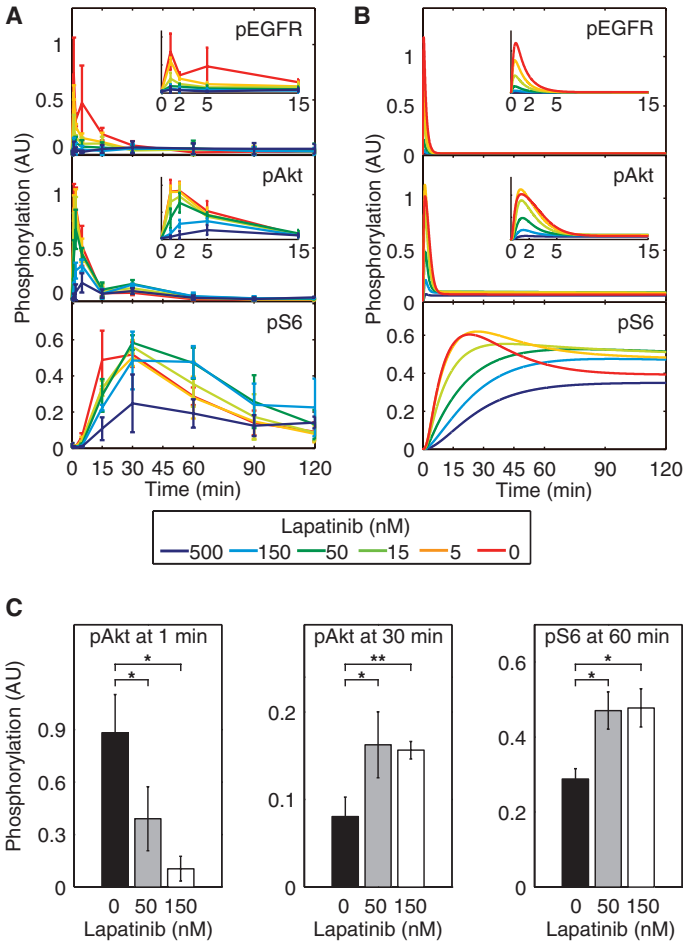

Fig. 7. Low-pass filter characteristic of the Akt pathway can convert an EGFR inhibitor into an activator of S6 phosphorylation. (**A**) After treatment with the indicated concentrations of lapatinib, an EGFR inhibitor, for 16 hours, the PC12 cells were stimulated with EGF (30 ng/ml) and the phosphorylation of the indicated proteins was measured. Means and SEM of three independent experiments are shown. The expanded time courses are shown in the insets. (**B**) In the simulation, the parameters of the inhibitor reactions with EGFR were fitted with the results of the experiments for the inhibitors in (A) (fig. S12). The same parameters downstream of pEGFR were used in Fig. 1 and fig. S2. The simulation results corresponding to the experiments in (A) are shown. The expanded time courses are shown in the insets. (**C**) Phosphorylation of Akt and S6 at the indicated times in the presence of the indicated concentrations of lapatinib. $^{*}P < 0.05$, $^{**}P < 0.01$ (Student's *t* test).

DISCUSSION

We found that a strong transient time course of an upstream molecule poorly induced a downstream response, whereas a weak sustained time course of the upstream molecule strongly induced a downstream response (Fig. 8). This phenomenon can be explained by a low-pass filter characteristic of the pathway. The peak amplitudes of the transient and sustained time courses of the upstream molecule were mainly composed of higher- and lower-frequency waves, respectively (Figs. 4 and 8). When the cutoff frequency of a pathway was high, both the higher- and the lower-frequency waves of the upstream molecule were similarly transferred downstream. Therefore, the main-frequency waves were shared between the upstream and the downstream molecules. For this reason, the time courses of pEGFR and pAkt were similar, and the relationship between the peak amplitudes of the transient and sustained time courses of the upstream and the downstream molecules was coupled (Figs. 1 and 6 and fig. S11). However, when the cutoff frequency of a pathway was low, the higher-frequency waves were not efficiently transferred downstream relative to the lower-frequency waves. This phenomenon resulted in the relative enhancement of the lower-frequency waves, compared with the higher-frequency waves, at the downstream molecule. Therefore, the main-frequency waves of the upstream and downstream molecules were switched from higher- to lower-frequency waves. For this reason, the time courses of pAkt and pS6 differed, and the relationships between the peak amplitudes of the transient and sustained time courses of the upstream and downstream molecules were not always coupled (Figs. 1 and 6 and fig. S11). In particular, when the amplitude of the lower-frequency waves of the sustained time course was higher than that of the lower-frequency waves of the transient time course (Fig. 4B), the relationship of the peak amplitudes of the transient and sustained time courses between the upstream and downstream molecules could be decoupled.

Whether the relationship between the peak amplitudes of the transient and sustained time courses of the upstream and the downstream molecules was coupled or decoupled was determined by the cutoff frequency of the pathway and by the differences in the frequency waves of the transient and sustained time courses for the upstream molecule. We identified the critical parameters for the cutoff frequency in the Akt pathway model by the parameter sensitivity analysis (*27*) (fig. S13). The cutoff frequency of the pEGFR-to-pAkt part of the pathway was higher than that of the pAkt-to-pS6 part of the pathway, suggesting that a slower reaction exists in the pAkt-to-pS6 portion rather than in the pEGFR-to-pAkt portion of the pathway in PC12 cells.

The time course of EGF in vivo is unknown; however, we expect that the biological function of the low-pass filter characteristic of the Akt pathway may be related to the downstream function. Phosphorylation of S6, one of the components of ribosome, correlates with ribosome biogenesis and protein synthesis (*28*), processes that consume most of a growing cell's energy (*29*) and that take ~30 min (*30*). One could predict that if the signal continued for <30 min, then ribosome biogenesis and protein synthesis would not be completed and the energy would be wasted. Because of the low-pass filter characteristic, the Akt pathway would only transmit upstream signals with a sufficient duration for the completion of the processes and would filter out signals with a shorter duration.

A low-pass filter characteristic is not limited to the Akt pathway; a biochemical reaction can be approximated by a consecutive reaction, which is a typical low-pass filter, under unsaturated conditions (fig. S6D)

(*7*–*9*, *31*, *32*). Therefore, it is possible that chains of a biochemical reaction, including signaling pathways, also exhibit a low-pass filter characteristic. Although we featured the decoupling effect by a low-pass filter characteristic, a low-pass filter with a high cutoff frequency can exhibit high-fidelity transmission as seen in the pEGFR-to-pAkt pathway, for which the signal intensities were coupled. Therefore, even though signal intensities between upstream and downstream are coupled, one should be aware of the possibility that the pathway can serve as a low-pass filter. Additionally, it is also possible that other characteristics, such as a band-pass filter, emerge in chains of a biochemical reaction if these chains contain one or more feedback loops (*7*), and that not all downstream pathways of Akt may exhibit a low-pass filter characteristic.

Our finding raises a caution in interpreting the effects of pathway perturbations. If a pharmacological or genetic perturbation reduces the peak amplitude of a transient time course in a target pathway but increases that of a sustained time course in a pathway with low-pass filter characteristics, the downstream responses might be increased, rather than reduced. This effect can be opposite to the intuitively predicted effect. Consistent with this concept, we found that at certain concentrations, the EGFR inhibitor lapatinib acted as a downstream activator of pS6 because it converted the pAkt response from a transient time course to a sustained time course. Similar opposite effects of inhibitors have been previously reported: An integrin inhibitor, which is an antiangiogenic agent used as a cancer therapeutic, stimulated angiogenesis and tumor growth when administered at low concentrations (*33*). The presence of a low-pass filter in the integrin pathway may explain this contradictory effect. Indeed, in a pathway with low-pass filter properties, any inhibitor that can convert a strong transient time course into a weak sustained time course can be a potential downstream activator. Therefore, the effect of such a perturbation at an early step in a pathway should be determined through analysis of the relationship of the time courses between the upstream and downstream molecules and the cutoff frequency of the pathway, because the peak amplitude in the downstream effector may not reflect that of the upstream molecule.

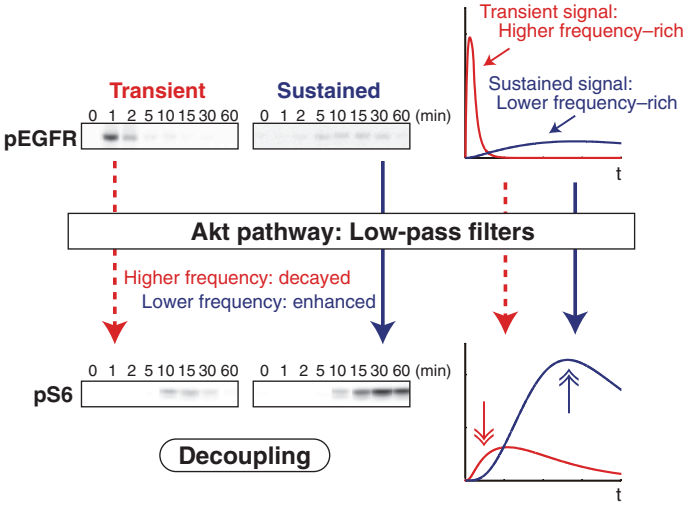

Fig. 8. Decoupling of the relationship of the peak amplitudes between pEGFR and pS6 by the low-pass filter characteristic of the Akt pathway. The peak amplitudes of EGFR and S6 phosphorylation were decoupled in PC12 cells; a weak sustained EGFR phosphorylation, rather than a strong transient phosphorylation, strongly induced S6 phosphorylation. The transient and sustained EGFR phosphorylation consisted of higher- and lower-frequency waves, respectively. Because the Akt pathway exhibited a low-pass filter characteristic, the higher-frequency waves were not efficiently transferred downstream relative to the lower-frequency waves. Thus, the Akt pathway serves as a low-pass filter, enabling the decoupling of EGFR phosphorylation and downstream effector phosphorylation.

Decoupling effects can also be seen in biological processes. For example, the process of gene expression exhibits a low-pass filter characteristic. In general, the time course of signal transduction is faster than that of gene expression (*30*, *34*). This observation suggests that the cutoff frequency of signal transduction is higher than that of gene expression; thus, only low-frequency waves, rather than high-frequency waves, of the time course of a signaling molecule are efficiently transferred to gene expression. Therefore, the relationship of the peak amplitudes between a signaling molecule and gene expression could be decoupled; in other words, a weak sustained time course of the signaling molecule might induce gene expression more strongly than a strong transient time course of the signaling molecule.

By step stimulation with EGF, the dose response of pAkt at 1 min was monotonic, whereas that of pS6 at 30 min was convex (Fig. 1, B and C, left columns, and fig. S3). The dose response of pAkt at 1 min in the high-frequency waves, which mainly constituted the peak amplitude, was monotonic, whereas the sustained response at 30 min in the lower-frequency waves was convex (fig. S11A). The main-frequency waves of pAkt and pS6 were switched from high- to low-frequency waves, resulting in a convex dose response of pS6 at 30 min. The switching of the main-frequency waves between the upstream and the downstream molecules is responsible for both the decoupling effect and the convex dose response. Indeed, EGF has been reported to trigger a convex dose response in various cellular processes, such as DNA synthesis in corneal fibroblasts (*35*), corneal wound healing (*36*), and proliferation in endometrial carcinoma (*37*). Our finding of a low-pass filter in the EGFR pathway may explain these in vivo responses.

Similar frequency response analyses of signaling cascades have been used to investigate osmotic adaptation in the Hog1 mitogen-activated protein kinase pathway of budding yeast (*7*, *8*), calcium signaling (*38*–*41*), and other studies (*9*, *31*, *32*). In these studies, periodic external stimuli were used for the frequency response analysis; however, external stimuli are not always effective for frequency response analyses because such analyses require a linear relationship between the upstream and the downstream molecules. Consequently, frequency response analyses cannot be directly used under conditions where the relationship is not linear, such as when the binding of growth factors to receptors becomes saturated at high concentrations of growth factors. To avoid the saturation of growth factor and receptor interactions, we analyzed the responses of the molecules downstream of the receptors. In addition, producing periodic receptor phosphorylation can be technically difficult. Therefore, we obtained a periodic sine wave by decomposing the time course into sine waves with a Fourier transform and obtained the frequency-dependent gain by dividing the sine waves of upstream molecules by those of downstream molecules with the same frequency. This method can be potentially applied to any time course experiment examining signal transduction.

MATERIALS AND METHODS

Cell culture and immunoblotting

PC12 cells were provided by M. Nakafuku (Cincinnati Children's Hospital Medical Center, Cincinnati, OH). The cell culture and growth factor stimulation have been previously described (*6*). Lapatinib was purchased from Toronto Research Chemicals, and LY294002 and rapamycin were purchased from Sigma-Aldrich and Calbiochem, respectively. Antibodies

against pEGFR (Tyr[1068], no. 2234), pS6 kinase (Thr[389], no. 9206), total eIF4E (no. 9742), and PathScan Multiplex Western Cocktail I [antibodies against pAkt (Ser[473]), pS6 (Ser[235/236]), and total eIF4E (no. 5301)] were purchased from Cell Signaling Technology. Immunoblotting was performed with Immobilon Western Chemiluminescent HRP Substrate (Millipore). Ramp stimulation with EGF (Fig. 1) was performed with a microsyringe pump as previously described (*6*).

Processing of signal intensities of immunoblots

We detected the chemiluminescent signals of immunoblots with a luminoimage analyzer (LAS-4000; Fujifilm) and quantified chemiluminescent signals with the TotalLab TL120 analysis software (Nonlinear Dynamics). We obtained the signal intensities of pEGFR, pAkt, pS6, and eIF4E by quantifying immunoblot images. We normalized the signal intensities so that the peak intensity of each molecule was set at 1. We used a single gel and membrane for each of three independent experiments and obtained the signal intensities of pEGFR, pAkt, pS6, and total eIF4E simultaneously. We obtained the normalized intensity by dividing the raw intensities of pEGFR, pAkt, and pS6 by that of total eIF4E in the same lane as an internal control to obtain scaling factors, which were defined by the square root of the sum of squares of the normalized intensities for all points of each molecule in each experiment. The normalized intensities of each phosphorylated molecule were divided by the scaling factor for each molecule to obtain scaled intensity. The scaled intensities of three independent experiments for each growth factor were averaged and multiplied by the average of the scaling factor to obtain averaged intensities. Averaged intensities were divided by their maximum values.

Simulation and parameter estimation

We performed the simulation and parameter estimation with COPASI (*42*) (version 4.5) and also the simulation with Matlab (version R2008a; MathWorks). We estimated the parameters, using two methods in series, first with evolutionary programming to approximate the neighborhood of the local minimum followed by the Levenberg-Marquardt method to reach the local minimum. In these methods, the parameters were estimated to minimize the objective function value, which is defined as the sum of the square residuals between our measurements and the model trajectories. After 100 independent estimations for the Akt pathway model, we selected the model that had the minimum objective function value. Among the best 10 models, we also confirmed that the model had similar characteristics of the Akt pathway in terms of the time courses, dose responses, amplitude spectra, and frequency-dependent gain. This suggested that our finding did not depend on specific parameter conditions and that we captured general characteristics of the Akt pathway. The parameters and equations used in this study are shown in fig. S2. The block diagrams of the models were made by CellDesigner (*43*). The COPASI and SBML (*44*) files of our models are available on our Web site (http://www.kurodalab.org/info/Akt). The SBML files are also available to the public on the BioModels Database (*45*) (http://www.ebi.ac.uk/biomodels). BioModels Database IDs of the EGF-dependent Akt pathway model, the NGF-dependent Akt pathway model, and the inhibitor model are MODEL1004060001, MODEL1004060002, and MODEL1004060003, respectively.

For the parameter fitting, we used the experimental data obtained in response to step stimulation with EGF (Fig. 1, left columns). The data comprised 126 points consisting of six doses, seven time points, and three molecules. We further validated the model with additional experimental data in response to pulse and ramp stimulation with EGF (Fig. 1, middle and right columns). The data comprised 246 points consisting of six stimulation patterns and seven time points for the pulse stimulation and four patterns and 10 time points for the ramp stimulation.

Frequency response analysis

The time courses of the Akt pathway model were obtained from before 10 hours of stimulation until after 10 hours (stationary state) of stimulation with a 1-s sampling rate. The time courses of the Akt pathway model were subjected to Fourier transform with the Hanning window, and the absolute value was used as an amplitude spectrum. We defined the frequency-dependent gains as the quotient of the amplitude spectrum of a downstream molecule divided by that of an upstream molecule on the basis of the assumption that each pathway is a linear time-invariant system. We obtained similar frequency-dependent gains regardless of the stimulation patterns. The fitted consecutive reactions, which are linear time-invariant systems, reproduced the time courses of pEGFR, pAkt, and pS6 by step, pulse, and ramp stimulation (fig. S8). These findings indicate that a consecutive reaction can retain the essential properties of the Akt pathway model and that the Akt pathway model can be approximated by a linear time-invariant model.

Amplitude spectra and phase spectra within the low-, middle-, and high-frequency bands were subjected to an inverse Fourier transform, and the time courses of the low-, middle-, and high-frequency waves were reconstituted.

Fitting of the Akt pathway model as a simple consecutive reaction

We defined a simple consecutive reaction from $x(t)$ to $y(t)$, which is a series of first-order reactions, as follows:

$$\tau \frac{dy(t)}{dt} = Kx(t) - y(t)$$

where K and τ denote a gain and a time constant, respectively. To fit the above equation with the Akt pathway model, we used the time courses of pEGFR and pAkt as $x(t)$ in an integral form of the equation and obtained pAkt and pS6 as $y(t)$, respectively. We determined K and τ by minimizing the square sum of the error between the time courses of the Akt model and $y(t)$.

SUPPLEMENTARY MATERIALS

www.sciencesignaling.org/cgi/content/full/3/132/ra56/DC1
Fig. S1. Gel images of immunoblots.
Fig. S2. Akt pathway model.
Fig. S3. Dose responses of pEGFR, pAkt, and pS6.
Fig. S4. EGF-dependent phosphorylation of S6K.
Fig. S5. Inhibition of S6 phosphorylation by LY294002 or rapamycin.
Fig. S6. Concept of frequency response analysis.
Fig. S7. Frequency response analysis of the Akt pathway model.
Fig. S8. Responses of the fitted consecutive reactions.
Fig. S9. NGF-dependent Akt pathway.
Fig. S10. NGF-dependent Akt pathway model.
Fig. S11. Time courses of the low-, middle-, and high-frequency waves of pEGFR, pAkt, and pS6.
Fig. S12. Inhibitor model.
Fig. S13. Parameter sensitivity analysis of EGF-dependent Akt pathway model.
Model files in COPASI (.cps) and SBML (.xml) format for the EGF-Akt pathway model, the NGF-Akt pathway model, and the inhibitor pathway model.

REFERENCES AND NOTES

1. B. P. Lathi, *Modern Digital and Analog Communication Systems* (Oxford Univ. Press, New York, ed. 3, 1998).
2. C. J. Marshall, Specificity of receptor tyrosine kinase signaling: Transient versus sustained extracellular signal-regulated kinase activation. *Cell* **80**, 179–185 (1995).
3. D. Bray, Protein molecules as computational elements in living cells. *Nature* **376**, 307–312 (1995).
4. B. N. Kholodenko, Cell-signalling dynamics in time and space. *Nat. Rev. Mol. Cell Biol.* **7**, 165–176 (2006).
5. M. Behar, H. G. Dohlman, T. C. Elston, Kinetic insulation as an effective mechanism for achieving pathway specificity in intracellular signaling networks. *Proc. Natl. Acad. Sci. U.S.A.* **104**, 16146–16151 (2007).

6. S. Sasagawa, Y. Ozaki, K. Fujita, S. Kuroda, Prediction and validation of the distinct dynamics of transient and sustained ERK activation. *Nat. Cell Biol.* **7**, 365–373 (2005).
7. J. T. Mettetal, D. Muzzey, C. Gómez-Uribe, A. van Oudenaarden, The frequency dependence of osmo-adaptation in *Saccharomyces cerevisiae*. *Science* **319**, 482–484 (2008).
8. P. Hersen, M. N. McClean, L. Mahadevan, S. Ramanathan, Signal processing by the HOG MAP kinase pathway. *Proc. Natl. Acad. Sci. U.S.A.* **105**, 7165–7170 (2008).
9. M. R. Bennett, W. L. Pang, N. A. Ostroff, B. L. Baumgartner, S. Nayak, L. S. Tsimring, J. Hasty, Metabolic gene regulation in a dynamically changing environment. *Nature* **454**, 1119–1122 (2008).
10. I. Vivanco, C. L. Sawyers, The phosphatidylinositol 3-kinase–AKT pathway in human cancer. *Nat. Rev. Cancer* **2**, 489–501 (2002).
11. B. D. Manning, L. C. Cantley, AKT/PKB signaling: Navigating downstream. *Cell* **129**, 1261–1274 (2007).
12. K. Huff, D. End, G. Guroff, Nerve growth factor-induced alteration in the response of PC12 pheochromocytoma cells to epidermal growth factor. *J. Cell Biol.* **88**, 189–198 (1981).
13. A. N. Carter, C. P. Downes, Phosphatidylinositol 3-kinase is activated by nerve growth factor and epidermal growth factor in PC12 cells. *J. Biol. Chem.* **267**, 14563–14567 (1992).
14. M. Andjelković, H. S. Suidan, R. Meier, M. Frech, D. R. Alessi, B. A. Hemmings, Nerve growth factor promotes activation of the α, β and γ isoforms of protein kinase B in PC12 pheochromocytoma cells. *Eur. J. Biochem.* **251**, 195–200 (1998).
15. M. Kleijn, G. I. Welsh, G. C. Scheper, H. O. Voorma, C. G. Proud, A. A. Thomas, Nerve and epidermal growth factor induce protein synthesis and eIF2B activation in PC12 cells. *J. Biol. Chem.* **273**, 5536–5541 (1998).
16. J. Huang, B. D. Manning, The TSC1–TSC2 complex: A molecular switchboard controlling cell growth. *Biochem. J.* **412**, 179–190 (2008).
17. D. C. Fingar, J. Blenis, Target of rapamycin (TOR): An integrator of nutrient and growth factor signals and coordinator of cell growth and cell cycle progression. *Oncogene* **23**, 3151–3171 (2004).
18. S. Wullschleger, R. Loewith, M. N. Hall, TOR signaling in growth and metabolism. *Cell* **124**, 471–484 (2006).
19. D. A. Guertin, D. M. Sabatini, Defining the role of mTOR in cancer. *Cancer Cell* **12**, 9–22 (2007).
20. Y. Mamane, E. Petroulakis, O. LeBacquer, N. Sonenberg, mTOR, translation initiation and cancer. *Oncogene* **25**, 6416–6422 (2006).
21. I. Ruvinsky, N. Sharon, T. Lerer, H. Cohen, M. Stolovich-Rain, T. Nir, Y. Dor, P. Zisman, O. Meyuhas, Ribosomal protein S6 phosphorylation is a determinant of cell size and glucose homeostasis. *Genes Dev.* **19**, 2199–2211 (2005).
22. M. Björklund, M. Taipale, M. Varjosalo, J. Saharinen, J. Lahdenperä, J. Taipale, Identification of pathways regulating cell size and cell-cycle progression by RNAi. *Nature* **439**, 1009–1013 (2006).
23. M. Stolovich, H. Tang, E. Hornstein, G. Levy, R. Cohen, S. S. Bae, M. J. Birnbaum, O. Meyuhas, Transduction of growth or mitogenic signals into translational activation of TOP mRNAs is fully reliant on the phosphatidylinositol 3-kinase-mediated pathway but requires neither S6K1 nor rpS6 phosphorylation. *Mol. Cell. Biol.* **22**, 8101–8113 (2002).
24. W. S. Hlavacek, J. R. Faeder, M. L. Blinov, R. G. Posner, M. Hucka, W. Fontana, Rules for modeling signal-transduction systems. *Sci. STKE* **2006**, re6 (2006).
25. D. W. Rusnak, K. Affleck, S. G. Cockerill, C. Stubberfield, R. Harris, M. Page, K. J. Smith, S. B. Guntrip, M. C. Carter, R. J. Shaw, A. Jowett, J. Stables, P. Topley, E. R. Wood, P. S. Brignola, S. H. Kadwell, B. R. Reep, R. J. Mullin, K. J. Alligood, B. R. Keith, R. M. Crosby, D. M. Murray, W. B. Knight, T. M. Gilmer, K. Lackey, The characterization of novel, dual ErbB-2/EGFR, tyrosine kinase inhibitors: Potential therapy for cancer. *Cancer Res.* **61**, 7196–7203 (2001).
26. M. A. Fabian, W. H. Biggs III, D. K. Treiber, C. E. Atteridge, M. D. Azimioara, M. G. Benedetti, T. A. Carter, P. Ciceri, P. T. Edeen, M. Floyd, J. M. Ford, M. Galvin, J. L. Gerlach, R. M. Grotzfeld, S. Herrgard, D. E. Insko, M. A. Insko, A. G. Lai, J. M. Lélias, S. A. Mehta, Z. V. Milanov, A. M. Velasco, L. M. Wodicka, H. K. Patel, P. P. Zarrinkar, D. J. Lockhart, A small molecule–kinase interaction map for clinical kinase inhibitors. *Nat. Biotechnol.* **23**, 329–336 (2005).
27. R. Heinrich, S. Schuster, *The Regulation of Cellular Systems* (Chapman & Hall, New York, 1996).
28. O. Meyuhas, Physiological roles of ribosomal protein S6: One of its kind. *Int. Rev. Cell Mol. Biol.* **268**, 1–37 (2008).
29. E. V. Schmidt, The role of c-*myc* in cellular growth control. *Oncogene* **18**, 2988–2996 (1999).
30. U. Alon, *An Introduction to Systems Biology: Design Principles of Biological Circuits* (Chapman & Hall/CRC, New York, 2006).
31. P. B. Detwiler, S. Ramanathan, A. Sengupta, B. I. Shraiman, Engineering aspects of enzymatic signal transduction: Photoreceptors in the retina. *Biophys. J.* **79**, 2801–2817 (2000).
32. M. Samoilov, A. Arkin, J. Ross, Signal processing by simple chemical systems. *J. Phys. Chem. A* **106**, 10205–10221 (2002).
33. A. R. Reynolds, I. R. Hart, A. R. Watson, J. C. Welti, R. G. Silva, S. D. Robinson, G. Da Violante, M. Gourlaouen, M. Salih, M. C. Jones, D. T. Jones, G. Saunders, V. Kostourou, F. Perron-Sierra, J. C. Norman, G. C. Tucker, K. M. Hodivala-Dilke, Stimulation of tumor growth and angiogenesis by low concentrations of RGD-mimetic integrin inhibitors. *Nat. Med.* **15**, 392–400 (2009).
34. J. A. Papin, T. Hunter, B. O. Palsson, S. Subramaniam, Reconstruction of cellular signalling networks and analysis of their properties. *Nat. Rev. Mol. Cell Biol.* **6**, 99–111 (2005).
35. P. G. Woost, J. Brightwell, R. A. Eiferman, G. S. Schultz, Effect of growth factors with dexamethasone on healing of rabbit corneal stromal incisions. *Exp. Eye Res.* **40**, 47–60 (1985).
36. W. D. Mathers, M. Sherman, A. Fryczkowski, J. V. Jester, Dose-dependent effects of epidermal growth factor on corneal wound healing. *Invest. Ophthalmol. Vis. Sci.* **30**, 2403–2406 (1989).
37. M. Korc, C. A. Haussler, N. S. Trookman, Divergent effects of epidermal growth factor and transforming growth factors on a human endometrial carcinoma cell line. *Cancer Res.* **47**, 4909–4914 (1987).
38. R. E. Dolmetsch, R. S. Lewis, C. C. Goodnow, J. I. Healy, Differential activation of transcription factors induced by Ca^{2+} response amplitude and duration. *Nature* **386**, 855–858 (1997).
39. R. E. Dolmetsch, K. Xu, R. S. Lewis, Calcium oscillations increase the efficiency and specificity of gene expression. *Nature* **392**, 933–936 (1998).
40. T. Tomida, K. Hirose, A. Takizawa, F. Shibasaki, M. Iino, NFAT functions as a working memory of Ca^{2+} signals in decoding Ca^{2+} oscillation. *EMBO J.* **22**, 3825–3832 (2003).
41. P. De Koninck, H. Schulman, Sensitivity of CaM kinase II to the frequency of Ca^{2+} oscillations. *Science* **279**, 227–230 (1998).
42. S. Hoops, S. Sahle, R. Gauges, C. Lee, J. Pahle, N. Simus, M. Singhal, L. Xu, P. Mendes, U. Kummer, COPASI—a COmplex PAthway SImulator. *Bioinformatics* **22**, 3067–3074 (2006).
43. A. Funahashi, M. Morohashi, H. Kitano, N. Tanimura, CellDesigner: A process diagram editor for gene-regulatory and biochemical networks. *BIOSILICO* **1**, 159–162 (2003).
44. M. Hucka, A. Finney, H. M. Sauro, H. Bolouri, J. C. Doyle, H. Kitano, A. P. Arkin, B. J. Bornstein, D. Bray, A. Cornish-Bowden, A. A. Cuellar, S. Dronov, E. D. Gilles, M. Ginkel, V. Gor, I. Goryanin, W. J. Hedley, T. C. Hodgman, J. H. Hofmeyr, P. J. Hunter, N. S. Juty, J. L. Kasberger, A. Kremling, U. Kummer, N. Le Novère, L. M. Loew, D. Lucio, P. Mendes, E. Minch, E. D. Mjolsness, Y. Nakayama, M. R. Nelson, P. F. Nielsen, T. Sakurada, J. C. Schaff, B. E. Shapiro, T. S. Shimizu, H. D. Spence, J. Stelling, K. Takahashi, M. Tomita, J. Wagner, J. Wang, The systems biology markup language (SBML): A medium for representation and exchange of biochemical network models. *Bioinformatics* **19**, 524–531 (2003).
45. N. Le Novère, B. Bornstein, A. Broicher, M. Courtot, M. Donizelli, H. Dharuri, L. Li, H. Sauro, M. Schilstra, B. Shapiro, J. L. Snoep, M. Hucka, BioModels Database: A free, centralized database of curated, published, quantitative kinetic models of biochemical and cellular systems. *Nucleic Acids Res.* **34**, D689–D691 (2006).

46. **Acknowledgments:** We thank our laboratory members and N. Tanimura for critically reading this manuscript, R. Kunihiro for technical assistance, and M. Nakafuku (Cincinnati Children's Hospital Medical Center, Cincinnati, OH) for the PC12 cells. **Funding:** This work was supported by The Dynamic Mechanism of and Fundamental Technology for Biological System, CREST, Japan Science and Technology, and KAKENHI Scientific Research (A) (#21240025) from the Ministry of Education, Culture, Sports, Science and Technology of Japan, and a grant-in-aid from the Uehara Memorial Foundation. K.A.F. was supported by the Grant-in-Aid for the Global COE Program "Deciphering Biosphere from Genome Big Bang" from the Ministry of Education, Culture, Sports, Science and Technology of Japan. **Author contributions:** K.A.F. and S.K. conceived and designed this study. K.A.F. and Y.T. performed and analyzed the experiments and simulation. K.A.F. conceived the application of Fourier transform to the frequency response analysis and implemented it with the assistance of S.U. and Y.T. Y.T. together with K.A.F. and S.K. conceived the decoupling effect of inhibitor. S.U. supported the data analysis. Y.T., S.U., Y.O., and H.K. supported the design of this study. K.A.F., Y.T., and S.K. wrote the manuscript. **Accession numbers:** BioModels Database MODEL1004060001 (EGF-dependent Akt pathway model), MODEL1004060002 (NGF-dependent Akt pathway model), and MODEL1004060003 (EGF inhibitor model).

Submitted 28 December 2009
Accepted 9 July 2010
Final Publication 27 July 2010
10.1126/scisignal.2000810
Citation: K. A. Fujita, Y. Toyoshima, S. Uda, Y.-i. Ozaki, H. Kubota, S. Kuroda, Decoupling of receptor and downstream signals in the Akt pathway by its low-pass filter characteristics. *Sci. Signal.* **3**, ra56 (2010).

Decoupling of Receptor and Downstream Signals in the Akt Pathway by Its Low-Pass Filter Characteristics

Kazuhiro A. Fujita, Yu Toyoshima, Shinsuke Uda, Yu-ichi Ozaki, Hiroyuki Kubota and Shinya Kuroda (July 27, 2010)

Science Signaling **3** (132), ra56. [doi: 10.1126/scisignal.2000810]

Science Signaling (ISSN 1937-9145) is published weekly, except the last December, by the American Association for the Advancement of Science, 1200 New York Avenue, NW, Washington, DC 20005.